ACS APPLIED MATERIALS & INTERFACES

Research Article

www.acsami.org

New Fluorescent and Colorimetric Probe for Cyanide: Direct Reactivity, High Selectivity, and Bioimaging Application

Xiaohong Cheng, Runli Tang, Huizhen Jia, Jun Feng, Jingui Qin, and Zhen Li*

Department of Chemistry, Hubei Key Lab on Organic and Polymeric Opto-Electronic Materials, Wuhan University, Wuhan 430072, China

Supporting Information

ABSTRACT: Taking advantage of the special nucleophilicity of cyanide, a new ratiometric fluorescent and colorimetric probe (**Coum-1**) was designed by tuning the π−conjugated bridge to affect the intramolecular charge transfer efficiency. Upon the addition of CN^- anion, the probe displayed very large blue-shift in both fluorescence (90 nm) and absorption (90 nm) spectra, with the detection limit of 800 nM. Other anions gave nearly no interference. Furthermore, **Coum-1** was successfully applied to the fluorescent microscopic imaging for the detection of CN^- in HeLa cells.

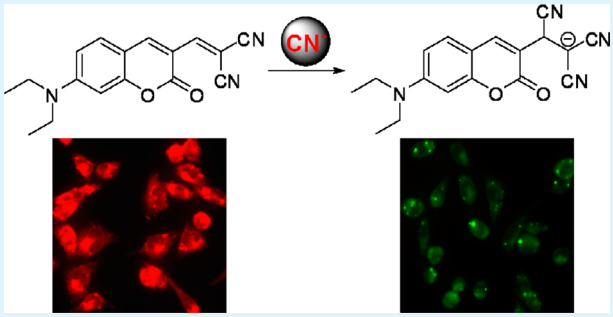

KEYWORDS: *probe, cyanide, reaction-based, intramolecular charge transfer, ratiometric fluorescent, cell imaging*

INTRODUCTION

The sensitive and selective detection of cyanide is becoming an increasing demand, because of the extreme toxicity of cyanide in physiological systems, as well as the continuing environmental concern caused by its widespread industrial use.[1−4] Various methods have been reported to analyze cyanide, especially as optical probes possessing innate advantages over others, for their high sensitivity, specificity, simplicity of implementation, and fast response times. Thanks to the enthusiastic efforts of scientists, some good fluorescent and colorimetric probes have been developed for the sensitive and selective detection of cyanide.[5−11] However, the reports concerning the bioimaging applications in living cells for cyanide were still very scarce.[12−14]

As to the design of optical probes, ratiometric method is becoming more promising, because it can enable the measurement of optical intensities at two different wavelengths, providing a built-in correction for environmental effects and increasing the dynamic range of measurement. This method is considered as a good approach to overcome the major limitation of intensity-based probes, in which variations in the environmental sample and probe distribution were problematic for quantitative measurements. However, the ratiometric fluorescence and colorimetric probes for cyanide, so far, are limited.[15,16]

Generally, ratiometric probes can be designed mainly according to two mechanisms: fluorescence resonance energy transfer (FRET) and intramolecular charge transfer (ICT).[17−22] Compared to the former, ICT-based ratiometric probes are structurally simple. For a typical ICT fluorescence probes, the tuning of the normal D/π/A structure of fluorophores would lead to different optical nature and concomitant fluorescent or/and color changes.[23] Thus, if some specific analyte could induce the structural tuning, then, this property could be employed to devise probes with high selectivity for the special analyte (Scheme 1).

In recent years, we attempted to develop novel ICT-based chemosensors by tuning the "push-and-pull" structure of fluorophores. As shown in Scheme 1a, the thioacetal moieties might be regarded as a weak electron donor, which could be converted to the electron-withdrawing aldehyde group in the presence of Hg^{2+}. This transformation from D-π-D′ to D-π-A could lead to the changes of the whole electronic property and ICT efficiency of the sensing system, accompanying with the corresponding fluorescent changes. Thus, this selective reaction could be considered as a new method to design ICT probes for the detection of Hg^{2+}.[24−27] By utilizing its affinity toward copper, we developed an indirect strategy to detect cyanide.[28−32] In the specific case (Scheme 1b), copper ions could coordinate with the electron donor moiety of the sensor molecule and the original strong electronic donor was converted into a weak one with the largely reduced donating ability to participate the ICT process. However, the added cyanide could preferentially snatch copper ions in the above complex to form stable $[Cu(CN)_x]^{n-}$ species. As a result, the liberated donor moiety of the sensor molecule recovered its electron-donating ability with obvious color changes from yellow to red. Different from these two approaches, here, we were wondering whether chemosensors with good performance could be designed by regulating the conjugated bridge to affect

Received: June 9, 2012
Accepted: July 20, 2012
Published: July 20, 2012

   dx.doi.org/10.1021/am3010412 | ACS Appl. Mater. Interfaces 2012, 4, 4387−4392

Scheme 1. General Strategies to Develop ICT-Based Chemosensors: (a) D-π-D′ to D-π-A; (b) D′-π-A to D-π-A; (c) D-π-A to D-π′-A

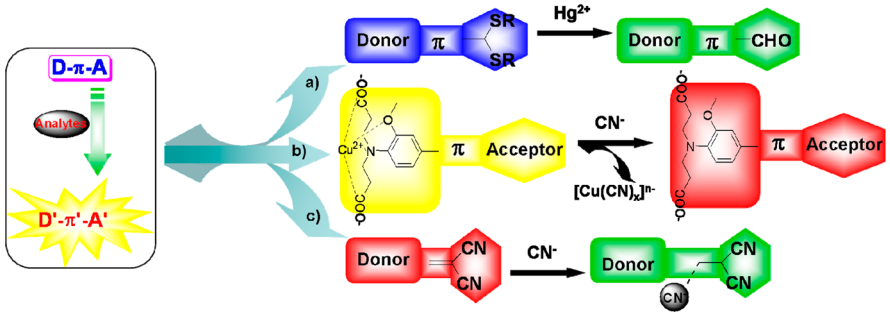

the ICT efficiency, resulting in the induced fluorescent and color changes.

After checking the literature carefully, we found that chemodosimetric sensors relied on the special nucleophilicity of cyanide was promising owing to their high selectivity.[33−38] The nucleophilic addition reaction between cyanide and the dicyano-vinyl group would break the conjugation of the electron donor and acceptor, thus, affecting the ICT efficiency and optical properties of the sensing system (Scheme 1c). If it was the case, this approach should be a new one for the development of new ICT-based chemosensors by tuning the "D-π-A" structure.

In the preliminary work from our laboratory, we reported an azobenzene structure as a ratiometric colorimetric chemodosimeter toward cyanide based on the special nucleophilicity of cyanide.[39] Here, in a continuation of the previous work, we designed a coumarin-malononitrile compound (**Coum-1**) as a fluorescent chemodosimeter toward cyanide, in which the two units of donor and acceptor were covalently linked through a double bond. The probe possessed coumarin as the fluorophore and a dicyano-vinyl group as a putative cyanide-dependent reactive subunit. **Coum-1** was red in color and emitted strong red fluorescence with the quantum yield of ∼0.45. Then, it was expected that cyanide could attack the α-position of the dicyano-vinyl group in **Coum-1**, to generate the stabilized anionic specie of **Coum-2**, which was yellow in color and emitted green fluorescence with the quantum yield of ∼0.33 (Scheme 2). If it was the case, the effective conjugation of the

Scheme 2. Structure of Coum-1 and the Sensing Process

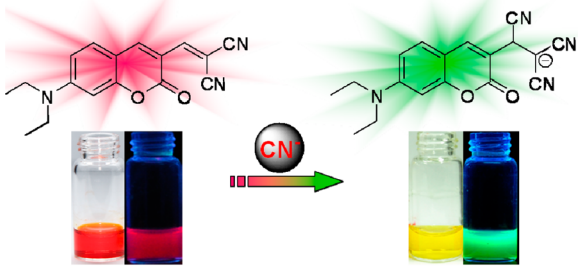

whole molecule of **Coum-1** should be broken, as a result, the electronic structure and optical properties would be changed. If cyanide anion was the unique nucleophile capable of inducing these changes, then, **Coum-1** could act as a cyanide-selective probe. Herein, we would like to describe the new ratiometric optical probe for cyanide in detail, featuring advantages such as relative good solubility in aqueous media, good ratiometric response, as well as the successful application in bioimaging of living cells.

MATERIALS AND INSTRUMENTATIONS

Ethanol was dried over and distilled from Na under an atmosphere of dry nitrogen. Triethylamine (Et_3N) was distilled under normal pressure and kept over potassium hydroxide. All other reagents were of analytical grade and used without further purification. Doubly distilled water was used in all experiments.

The ^1H and ^{13}C NMR spectra were measured on Varian Mercury300 spectrometer. Elemental analyses were performed by a CARLOERBA-1106 microelemental analyzer. Photoluminescence spectra were performed on a Hitachi F-4500 fluorescence spectrophotometer. UV−vis spectra were obtained using a Shimadzu UV-2550 spectrometer. The pH values were determined by using a DELTA 320 PH dollar.

Synthesis of 2-((7-(Diethylamino)-2-oxo-2H-chromen-3-yl)-methylene)malononitrile (Compound Coum-1). Under an atmosphere of dry argon, aldehyde-coumarin (**Coum-0**, 122.5 mg, 0.5 mmol) and malononitrile (66 mg, 1.0 mmol) were refluxing in absolute ethanol (6 mL) overnight with trace Et_3N as catalyst. Then, the resultant mixture was cooled to room temperature and the solvent was removed under reduced pressure. The resultant residue was purified by silica gel column chromatography using petroleum ether/dichloromethane (1/7, v/v) as eluent to afford coumarin-malonitrile (**Coum-1**) as a deep red solid (60 mg, 41.5%). ^1H NMR (300 MHz, DMSO-d_6) δ (ppm): 8.61 (s, 1H, −CH═C−), 8.01 (s, 1H, ArH), 7.64−7.61 (d, 1H, J = 9.0 Hz, ArH), 6.89−6.86 (d, 1H, J = 9.0 Hz, ArH), 6.67 (s, 1H, ArH), 3.59−3.52 (q, 4H, J = 7.0 Hz, $-CH_2-$), 1.14−1.18 (t, 6H, J = 6.0 Hz, $-CH_3$). ^{13}C NMR (75 MHz, DMSO-d_6) δ (ppm): 159.7, 158.7, 155.0, 154.1, 146.3, 133.6, 115.9, 114.5, 111.9, 110.2, 109.0, 97.5, 76.1, 45.6, 13.1. $C_{17}H_{15}N_3O_2$ (EA) (%, found/calcd): C, 69.19/69.61; H, 5.51/5.15; N, 14.45/14.33.

Preparation of Solutions of Anions. One mmol of inorganic salt ($NaOAc·3H_2O$, $NaNO_2$, $NaNO_3$, Na_2SO_3, NaF, Na_2CO_3, Na_2SO_4, Na_3PO_4, NaCl, $NaIO_3$, $KClO_3$, KBr, $Na_2HPO_4·12H_2O$, $NaHSO_3$, Na_2S, $Na_2S_2O_3·5H_2O$, NaI, KSCN, and NaCN) were dissolved in distilled water (10 mL) to afford 1×10^{-1} mol/L aqueous solution. The stock solutions were diluted to desired concentrations with water when needed.

Fluorescence and UV Absorption Changes of Coum-1 by CN^-. A solution of **Coum-1** (10 μM and 20 μM) was prepared in THF-H_2O solution (5:5, v/v, 10 mM HEPES, pH 7.04). Then 3.0 mL of the solution of **Coum-1** was placed in a quartz cell (10.0 mm width) and the fluorescent and absorption spectra were recorded. The NaCN aqueous solution was introduced in portions and the fluorescent and absorption changes were recorded at room temperature each time.

Fluorescence and UV Absorption Changes of Coum-1 by Other Anions. A solution of **Coum-1** (10 μM and 20 μM) was prepared in THF-H_2O solution (5:5, v/v, 10 mM HEPES, pH 7.04). Then 3.0 mL of the solution of **Coum-1** was placed in a quartz cell (10.0 mm width) and the fluorescent and absorption spectra were

dx.doi.org/10.1021/am3010412 | ACS Appl. Mater. Interfaces 2012, 4, 4387−4392

recorded. Different anion solutions were introduced and the fluorescent and absorption changes were recorded at room temperature each time.

Cell Culture. HeLa cells were seeded to the 24-well plates, the cells with an initial density of 5×10^4 cells well^{-1} in 24-well plates were routinely maintained at 37 °C in a humidified 5% CO_2 atmosphere using DMEM (Dulbecco's modified eagle's medium) supplemented with 10% fetal bovine serum and 1% penicillin-streptomycin for 24 h.

Fluorescence Imaging. Fluorescence cell imaging was performed with an OLYMPUS IX71 scanning microscopy with a 40× objective lens. Fluorescence images of **Coum-1**-loaded cells were monitored at 460−490 nm and 510−550 nm for green and red channels, respectively. The data were analyzed using software package provided by OLYMPUS instruments. Before the experiments, cells were washed with PBS buffer and then incubated with **Coum-1** (100 μM) in PBS/DMSO (10/1, v/v) for 30 min. Cell imaging was then carried out after washing cells with PBS.

RESULTS AND DISCUSSION

Synthesis and Structural Characterization. The synthetic route to **Coum-1** was depicted in Scheme S1 in the Supporting Information. The target compound was prepared conveniently through the general Knoevenagel condensation reaction between **Coum-0** and malononitrile, following the similar procedure in the reported literature.[40] The synthetic route was simple and the purification was easy.

Coum-1 exhibited good solubility in common organic solvents, such as acetone, DMF, DMSO, CH_3CN, and THF. Its structure was well characterized by ^1H, ^{13}C NMR, and elemental analysis, and all gave satisfactory spectral data.

Optimization of Experimental Conditions. Experimental conditions including the optimum excitation wavelength, pH value, reaction media, and the time course were optimized. As to **Coum-1**, the maximum excitation wavelength was at about 520 nm, however, after the addition of excess of cyanide, the maximum excitation wavelength of the resultant anionic specie of **Coum-2** shifted to 415 nm. To obtain a ratiometric optical probe for cyanide as mentioned above, we chose 447 nm as the optimum excitation wavelength (see Figure S1d in the Supporting).

Figure S2 in the Supporting Information depicted the effect of pH values on the emission intensities of **Coum-1** and **Coum-1**+CN^-. It was obvious that the detection of **Coum-1** for CN^- anions could be operated in a wide pH range of 6−8. In the titration experiment, we chose the pH value of 7.04 by using the HEPES buffer for the purpose of physiological application.

Considering that **Coum-1** was not soluble in water completely, a portion of THF was added as a cosolvent. As shown in Figure S3c in the Supporting Information, with the fraction of THF of 50% (v/v), two well-separated emission peaks before and after the addition of cyanide could be obtained. Therefore, a reaction medium of 10 mM HEPES buffer (pH 7.04) containing 50% (v/v) THF was chosen for the reaction.

Because the optical signal changes relied on the chemical reaction between **Coum-1** and cyanide, the reaction rate might affect the experimental results. We investigated the influence of the reaction time on the sensing results, with the obtained results summarized in Figures S4 and S5 in the Supporting Information. When the concentration of CN^- was 0.5 equiv of **Coum-1**, a plateau of fluorescent intensity could be achieved after 30 min. With the increasing of the concentration of cyanide, such as 1.5 equiv, only 17 min were needed to achieve a plateau. The kinetic profiles of the fluorescent spectra at 495 nm were summarized in Figure S6 in the Supporting Information, and the first-order reaction rate constant could be calculated to be 1.48×10^{-3} S^{-1}. So, in the titration experiment, we measured the optical intensity changes of the **Coum-1** solutions 30 min later after all the species were added.

Sensing Properties. The sensing behavior of **Coum-1** toward cyanide was investigated carefully under the optimized condition. As shown in Figure 1, while the concentration of

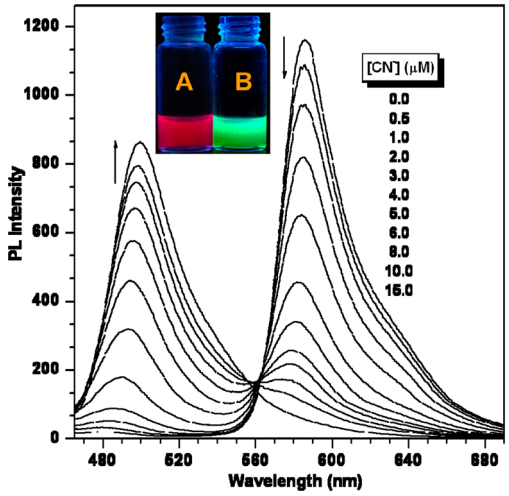

Figure 1. Fluorescent spectra of **Coum-1** (10 μM, in THF/HEPES = 5/5, pH 7.04) in the presence of different concentrations of CN^- excited at 447 nm. Inset: fluorescent photograph of (A) **Coum-1** and (B) **Coum-1** + CN^-.

CN^- was increased, the emission maximum shifted from 585 to 495 nm with a well-defined isoemissive point at 562 nm. Correspondingly, the fluorescence color changed from red to green (Figure 1, inset), which could be easily distinguished by the naked eyes under the aid of a normal UV lamp. Thus, the cyanide-promoted addition reaction of **Coum-1** occurred as expected, and the optical change was observed.

To see the sensing process more visually, we compared the intensities at different wavelengths of 495 and 585 nm, with the results summarized in Figure 2. It was easily seen that the intensity change was almost linear with the concentrations of CN^-. The detection limit could be determined to be 800 nM,[41] which was much lower than the maximum contaminant level (MCL) for cyanide in drinking water (2.7 μM) set by the World Health Organization (WHO).[42] It should be pointed out that the difference between the two emission wavelengths was very large (emission shift: $\Delta\lambda$ = 90 nm), which not only contributed to the accurate measurement of the intensities of the two emission peaks, but also resulted in a huge ratiometric value. In the presence of 1.0 equiv of CN^-, a ca. 470-fold enhancement in the ratiometric value of I_{495}/I_{585} (from 0.02 to 9.46) was achieved. The inset photos in Figure 2 showed that although not so sensitive as measured by the fluorescent spectrometer, we could easily distinguish the fluorescent color change upon the addition of as little as 20 μM of CN^- (the inset of Figure 2C).

Furthermore, the fluorescent properties of **Coum-1** with different concentration (5 μM) were studied in detail to check the reproducibility of the sensing behavior of **Coum-1** toward CN^- anions (Figure S7−S8). As shown in Figure S7, the fluorescent intensity of **Coum-1** apparently changed even at the concentration of CN^- as low as 1.5 μM. The inset pictures in

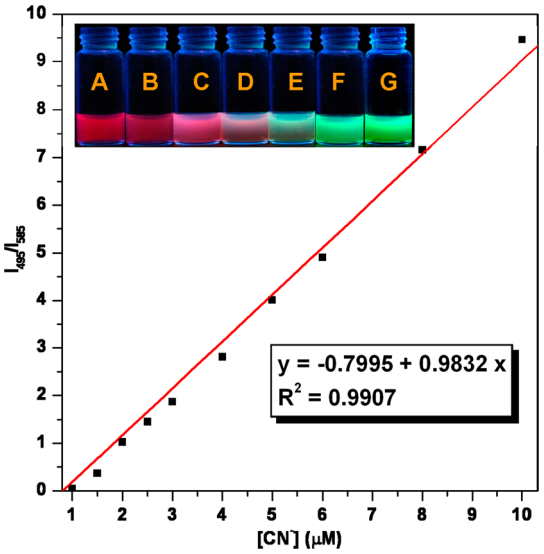

Figure 2. Ratiometric calibration curve I_{495}/I_{585} of **Coum-1** (10 μM, in THF/HEPES = 5/5, pH 7.04) as a function of the concentration of CN^-. Inset: fluorescent photograph of (A) **Coum-1** (100 μM) and (B–G) **Coum-1** + CN^-: (B) 10 μM, (C) 20 μM, (D) 50 μM, (E) 80 μM, (F) 100 μM, (G) 150 μM).

Figure S8 showed that we could easily distinguish the fluorescent color change upon the addition of as little as 10 μM CN^- (the inset of Figure S8D in the Supporting Information) with the aid of a normal UV lamp, indicating that **Coum-1** was a highly sensitive ratiometric fluorescent probe for CN^-.

To evaluate the specificity of **Coum-1** toward CN^-, various anions were examined in parallel under the same conditions. As shown in Figure 3 and Figure S9 in the Supporting Information, while the reaction of **Coum-1** with CN^- gave dramatic changes, AcO^-, NO_2^-, NO_3^-, SO_3^{2-}, F^-, CO_3^{2-}, SO_4^{2-}, PO_4^{3-}, Cl^-, IO_3^-, ClO_3^-, Br^-, HPO_4^{2-}, HSO_3^-, S^{2-}, $S_2O_3^{2-}$, and I^- caused no changes, except a negligible disturbance from SCN^-. These results further confirmed that

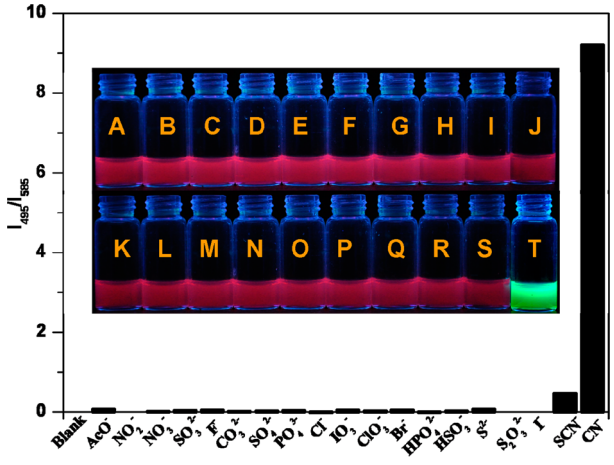

Figure 3. Fluorescent emission changes of **Coum-1** (10 μM, in THF/HEPES = 5/5, pH 7.04) in the presence of different anions (CN^-, 15 μM; others, 50 μM). Inset: fluorescent photograph of **Coum-1** to various anions. (A) **Coum-1**; (B–T)**Coum-1** + AcO^-, NO_2^-, NO_3^-, SO_3^{2-}, F^-, CO_3^{2-}, SO_4^{2-}, PO_4^{3-}, Cl^-, IO_3^-, ClO_3^-, Br^-, HPO_4^{2-}, HSO_3^-, S^{2-}, $S_2O_3^{2-}$, I^-, SCN^-, CN^-.

only cyanide could induce apparent fluorescent changes. That was to say, **Coum-1** could act as a cyanide-specific optical sensor.

In addition to the changed fluorescent behavior caused by the tuned D-π-A structure of **Coum-1** in the presence of cyanide, the color change was another apparent phenomenon. With the increasing concentrations of CN^-, the strong absorption band of **Coum-1** centered at 535 nm gradually decreased along with the appearance of a new absorption band centered at 445 nm. This absorption was responsible for the color change (from red to yellow) and perceptible to the naked eyes (the inset of Figure 4). Actually, apparent change in

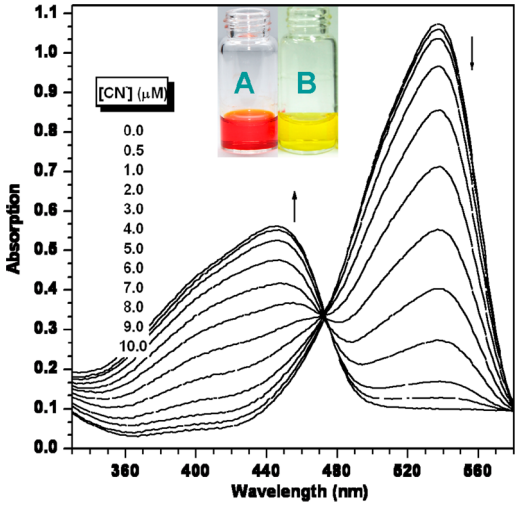

Figure 4. UV–vis spectra of **Coum-1** (20 μM, in THF/HEPES = 5/5, pH 7.04) in the presence of different concentrations of CN^-. Inset: photograph of (A) **Coum-1** and (B) **Coum-1** + CN^-.

absorption occurred even at the concentration of cyanide as low as 2 μM. From Figure S10 in the Supporting Information, it was easily seen that the intensity change was almost linear to the concentrations of the cyanide anion. More importantly, we could easily distinguish the color change at the concentration of CN^- as low as 10 μM (the inset of Figure S10 in the Supporting Information, the bottom, D) by the naked eyes. Meanwhile, the selective nature was investigated under the same conditions. As demonstrated in Figure S11 in the Supporting Information, only CN^- led to the apparent color changes, indicating that **Coum-1** had selective response toward CN^- over other anions. These results validated our design of ratiometric optical chemosensor toward cyanide, based on the nucleophilic addition reaction between cyanide and the dicyano-vinyl group.

Cell Imaging. The application of **Coum-1** to track intracellular CN^- levels was also conducted *via* a scanning microscopy. As shown in Figure 5, the **Coum-1**-loaded cells showed intracellular fluorescence at an emission channel collected at ~590 nm (the red channel), indicating that **Coum-1** could penetrate the cell membrane and be used for imaging of CN^- in living cells. Before the imaging experiment, the cells were treated with 100 μM NaCN aqueous solution for 20 min, followed by subsequent staining with **Coum-1** (100 μM, 30 min) in PBS/DMSO (10/1, v/v), and then washed with phosphate-buffered saline (PBS, 10 mM, pH 7.12) for three times. By virtue of a scanning microscopy, we could find that the emission intensity collected at the wavelength of ~590

dx.doi.org/10.1021/am3010412 | ACS Appl. Mater. Interfaces 2012, 4, 4387–4392

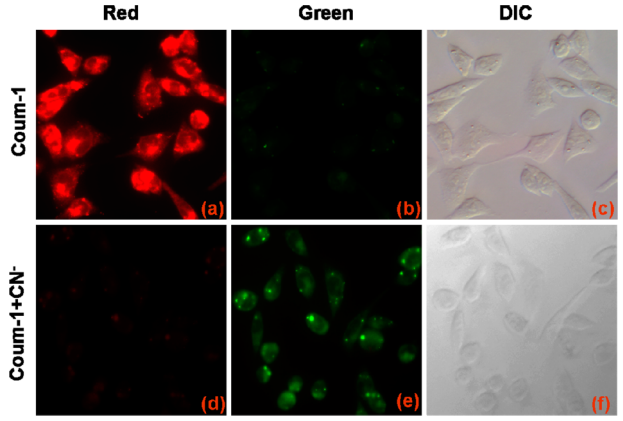

Figure 5. Scanning microscopic images of HeLa cells incubated with **Coum-1** and **Coum-1** upon treatment of CN^-.

nm (the red channel) decreased, whereas the intensity at ~520 nm (the green channel) increased. These were consistent with the observations in titration experiments and demonstrated that **Coum-1** could readily detect the CN^- in cells with the ratiometric fluorescent method.

Investigation of Sensing Mechanism. To explore the sensing mechanism of **Coum-1** to CN^-, the reaction mixture of **Coum-1** and CN^- was characterized by ^1H NMR spectra spectrometry. The partial ^1H NMR spectra of **Coum-1** and the resultant complex of **Coum-1** and CN^- (as its tetra-butylammpnium salts) were shown in Figure 6. The resonance signal at δ = 9.85 ppm was ascribed to the vinylic proton (H_a). Upon the addition of 0.5 equiv of CN^-, five new sets of signals appeared approximately of the same intensity with the integrated proportion of the original signals, while a new signal at 5.51 ppm appeared corresponding to the α-proton (H_b). This indicated that half of the dicyano-vinyl moiety in **Coum-1** had reacted with the added CN^-. After the addition of excess of CN^-, it was obvious that the resonance signal corresponding to the vinylic proton (H_a) at 9.85 ppm completely disappeared, while a new signal of the α-proton (H_b) appeared at 5.51 ppm. Meanwhile, the aromatic proton displayed obvious upfield shift compared to those of **Coum-1**, due to the broken conjugation bridge.

To get an insight into the molecular structure and the different optical behavior of **Coum-1** before and after the addition of CN^-, density functional theory (DFT) calculations were carried out at the B3LYP/6-31G(d) level by using Gaussian 09, Revision A.02 program.[43] The optimized structures of **Coum-1** and **Coum-1** + CN^- were shown in Figure 7. As to **Coum-1**, there was a conjugated bridge (−C═C−) between the coumarin (the donor) and dicyano groups (the acceptor), and the dihedral angle between the donor and the acceptor moiety was only 28°. After reacted with CN^-, the previous conjugated bridge (−C═C−) in **Coum-1** was transformed into a saturated bridge (−C−C−), and the dihedral angle became as large as 77°. These results partially proved that the blue-shifted emission and absorption of **Coum-1** upon the addition of cyanide should be ascribed to the weakened ICT process. Thus, the calculated results were in well accordance with the design concept of regulating the π-conjugated bridge, to affect the ICT efficiency and induce the fluorescent and color changes.

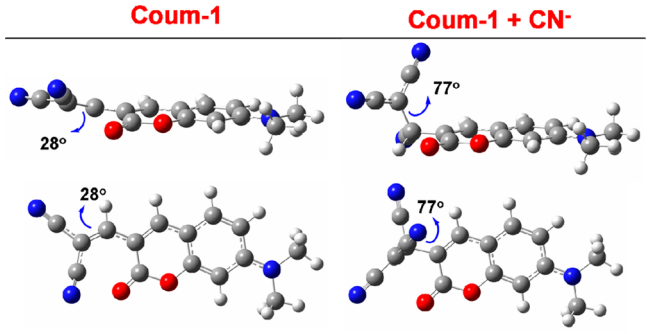

Figure 7. Optimized structures of **Coum-1** and **Coum-1** + CN^-.

CONCLUSIONS

A new ratiometric fluorescent and colorimetric probe (**Coum-1**) toward cyanide was designed based on the nucleophilic addition of cyanide to the α-position of dicyano-vinyl group. The probe demonstrated some advantages such as good sensitivity and high selectivity for CN^-, relative good solubility in aqueous media, good ratiometric response, as well as the successful application in bioimaging. The design approach in this work provided some useful information for the development of ratiometric optical probes. Further study is still in progress in our laboratory.

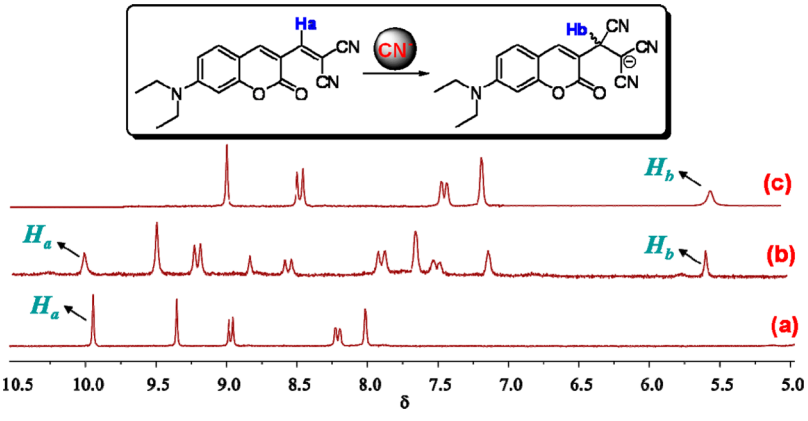

Figure 6. ^1H NMR spectra of: (a) **Coum-1**, (b) **Coum-1** + CN^- (0.5 equiv), and (c) **Coum-1** + CN^- (excess) as its tetra-butylammonium salts in DMSO-d_6.

dx.doi.org/10.1021/am3010412 | ACS Appl. Mater. Interfaces 2012, 4, 4387−4392

■ ASSOCIATED CONTENT

Supporting Information

The fluorescence spectra, the absorption spectra and ^{1}H and ^{13}C NMR spectra. This material is available free of charge via the Internet at http://pubs.acs.org.

■ AUTHOR INFORMATION

Corresponding Author

*Phone: 86-27-62254108. Fax: 86-27-68756757. E-mail: lizhen@whu.edu.cn or lichemlab@163.com.

Notes

The authors declare no competing financial interest.

■ ACKNOWLEDGMENTS

We are grateful to the NSFC (20974084), and the National Fundamental Key Research Program (2011CB932702) for financial support.

■ REFERENCES

(1) Xu, Z.; Chen, X.; Kim, H. N.; Yoon, J. *Chem. Soc. Rev.* **2010**, *39*, 127−137.
(2) Kim, D.-S.; Chung, Y.-M.; Jun, M.; Ahn, K. H. *J. Org. Chem.* **2009**, *74*, 4849−4854.
(3) Qian, G.; Li, X.; Wang, Z. *J. Mater. Chem.* **2009**, *19*, 522−530.
(4) Vallejos, S.; Estevez, P.; Garcia, F. C.; Serna, F.; de la Pena, J. L.; Garcia, J. M. *Chem. Commun.* **2010**, *46*, 7951−7953.
(5) Kim, H. J.; Ko, K. C.; Lee, J. H.; Lee, J. Y.; Kim, J. S. *Chem. Commun.* **2011**, *47*, 2886−2888.
(6) Peng, L.; Wang, M.; Zhang, G.; Zhang, D.; Zhu, D. *Org. Lett.* **2009**, *11*, 1943−1946.
(7) Lee, J. H.; Jeong, A. R.; Shin, I.-S.; Kim, H.-J.; Hong, J.-I. *Org. Lett.* **2010**, *12*, 764−767.
(8) Jung, H. S.; Han, J. H.; Kim, Z. H.; Kang, C.; Kim, J. S. *Org. Lett.* **2011**, *13*, 5056−5059.
(9) Chen, X.; Zhou, Y.; Peng, X.; Yoon, J. *Chem. Soc. Rev.* **2010**, *39*, 2120−2135.
(10) Xu, Z.; Kim, S. K.; Yoon, J. *Chem. Soc. Rev.* **2010**, *39*, 1457−1466.
(11) Chen, X.; Kang, S.; Kim, M. J.; Kim, J.; Kim, Y. S.; Kim, H.; Chi, B.; Kim, S.-J.; Lee, J. Y.; Yoon, J. *Angew. Chem., Int. Ed.* **2010**, *49*, 1422−1425.
(12) Chen, X.; Nam, S.-W.; Kim, G.-H.; Song, N.; Jeong, Y.; Shin, I.; Kim, S. K.; Kim, J.; Park, S.; Yoon, J. *Chem. Commun.* **2010**, *46*, 8953−8955.
(13) O'Neil, E. J.; Smith, B. D. *Coord. Chem. Rev.* **2006**, *250*, 3068−3080.
(14) Martínez-Máñez, R.; Sancenón, F. *Chem. Rev.* **2003**, *103*, 4419−4476.
(15) Divya, K. P.; Sreejith, S.; Balakrishna, B.; Jayamurthy, P.; Anees, P.; Ajayaghosh, A. *Chem. Commun.* **2010**, *46*, 6069−6071.
(16) Yu, H.; Fu, M.; Xiao, Y. *Phys. Chem. Chem. Phys.* **2010**, *12*, 7386−7391.
(17) Lv, X.; Liu, J.; Liu, Y.; Zhao, Y.; Chen, M.; Wang, P.; Guo, W. *Org. Biomol. Chem.* **2011**, *9*, 4954−4958.
(18) Long, L.; Lin, W.; Chen, B.; Gao, W.; Yuan, L. *Chem. Commun.* **2011**, *47*, 893−895.
(19) Yu, H.; Xiao, Y.; Guo, H.; Qian, X. *Chem.—Eur. J.* **2011**, *17*, 3179−3191.
(20) Wang, H.; Xue, L.; Qian, Y.; Jiang, H. *Org. Lett.* **2010**, *12*, 292−295.
(21) Saha, S.; Ghosh, A.; Mahato, P.; Mishra, S.; Mishra, S. K.; Suresh, E.; Das, S.; Das, A. *Org. Lett.* **2010**, *12*, 3046−3049.
(22) Yuan, L.; Lin, W.; Yang, Y.; Song, J.; Wang, J. *Org. Lett.* **2011**, *13*, 3730−3733.
(23) Liu, Z.; Wang, X.; Yang, Z.; He, W. *J. Org. Chem.* **2011**, *76*, 10286−10290.
(24) Cheng, X.; Li, Q.; Qin, J.; Li, Z. *ACS Appl. Mater. Interfaces* **2010**, *2*, 1066−1072.
(25) Cheng, X.; Li, Q.; Li, C.; Qin, J.; Li, Z. *Chem.—Eur. J.* **2011**, *17*, 7276−7281.
(26) Cheng, X.; Li, S.; Zhong, A.; Qin, J.; Li, Z. *Sens. Actuators B* **2011**, *157*, 57−63.
(27) Cheng, X.; Li, S.; Jia, H.; Zhong, A.; Zhong, C.; Feng, J.; Qin, J.; Li, Z. *Chem.—Eur. J.* **2012**, *18*, 1691−1699.
(28) Zeng, Q.; Cai, P.; Li, Z.; Qin, J.; Tang, B. *Chem. Commun.* **2008**, *44*, 1094−1096.
(29) Li, Z.; Lou, X.; Yu, H.; Li, Z.; Qin, J. *Macromolecules* **2008**, *41*, 7433−7439.
(30) Lou, X.; Zhang, L.; Qin, J.; Li, Z. *Chem. Commun.* **2008**, *44*, 5848−5850.
(31) Lou, X.; Qiang, L.; Qin, J.; Li, Z. *ACS Appl. Mater. Interfaces* **2009**, *1*, 2529−2535.
(32) Lou, X.; Qin, J.; Li, Z. *Analyst* **2009**, *134*, 2071−2075.
(33) Lee, C.-H.; Yoon, H.-J.; Shim, J.-S.; Jang, W.-D. *Chem.—Eur. J.* **2012**, *18*, 4513−4516.
(34) Wu, X.; Xu, B.; Tong, H.; Wang, L. *Macromolecules* **2011**, *44*, 4241−4248.
(35) Hong, S.-J.; Yoo, J.; Kim, S.-H.; Kim, J. S.; Yoon, J.; Lee, C.-H. *Chem. Commun.* **2009**, *45*, 189−191.
(36) Miyaji, H.; Kim, D.-S.; Chang, B.-Y.; Park, E.; Park, S.-M.; Ahn, K. H. *Chem. Commun.* **2008**, *44*, 753−755.
(37) Lee, H.; Chung, Y. M.; Ahn, K. H. *Tetrahedron Lett.* **2008**, *49*, 5544−5547.
(38) Sun, Y.; Wang, G.; Guo, W. *Tetrahedron* **2009**, *65*, 3480−3484.
(39) Cheng, X.; Zhou, Y.; Qin, J.; Li, Z. *ACS Appl. Mater. Interfaces* **2012**, *4*, 2133−2138.
(40) Kwon, H.; Lee, K.; Kim, H.-J. *Chem. Commun.* **2011**, *47*, 1773−1775.
(41) Shortreed, M.; Kopelman, R.; Kuhn, M.; Hoyland, B. *Anal. Chem.* **1996**, *68*, 1414−1418.
(42) *Guidelines for Drinking-Water Quality*, 3rd ed.; World Health Organization: Geneva, Switzerland, 2004.
(43) Frisch, M. J.; Trucks, G. W.; Schlegel, H. B.; Scuseria, G. E.; Robb, M. A.; Cheeseman, J. R.; Scalmani, G.; Barone, V.; Mennucci, B.; Petersson, G. A.; Nakatsuji, H.; Caricato, M.; Li, X.; Hratchian, H. P.; Izmaylov, A. F.; Bloino, J.; Zheng, G.; Sonnenberg, J. L.; Hada, M.; Ehara, M.; Toyota, K.; Fukuda, R.; Hasegawa, J.; Ishida, M.; Nakajima, T.; Honda, Y.; Kitao, O.; Nakai, H.; Vreven, T.; Montgomery, J. A.; Jr., Peralta, J. E.; Ogliaro, F.; Bearpark, M.; Heyd, J. J.; Brothers, E.; Kudin, K. N.; Staroverov, V. N.; Kobayashi, R.; Normand, J.; Raghavachari, K.; Rendell, A.; Burant, J. C.; Iyengar, S. S.; Tomasi, J.; Cossi, M.; Rega, N.; Millam, J. M.; Klene, M.; Knox, J. E.; Cross, J. B.; Bakken, V.; Adamo, C.; Jaramillo, J.; Gomperts, R.; Stratmann, R. E.; Yazyev, O.; Austin, A. J.; Cammi, R.; Pomelli, C.; Ochterski, J. W.; Martin, R. L.; Morokuma, K.; Zakrzewski, V. G.; Voth, G. A.; Salvador, P.; Dannenberg, J. J.; Dapprich, S.; Daniels, A. D.; Farkas, O.; Foresman, J. B.; Ortiz, J. V.; Cioslowski, J.; Fox, D. J. *Gaussian 09, Revision A.02*; Gaussian, Inc.: Wallingford CT, 2009.